



# Grain growth in electroplated (111)-oriented nanotwinned Cu

Yi-Sa Huang, Chien-Min Liu, Wei-Lan Chiu and Chih Chen\*

Department of Materials Science and Engineering, National Chiao Tung University, Hsinchu 30010, Taiwan, Republic of China

Received 3 December 2013; revised 26 May 2014; accepted 6 June 2014

Available online 18 June 2014

The grain growth of pulse-plated (111)-oriented nanotwinned Cu (nt-Cu) was investigated at 200–350 °C. The results indicate that after the annealing, the nt-Cu exhibits good thermal stability, and columnar grains with a (111)-oriented nt-Cu structure are maintained up to 300 °C. The columnar grains consume the original fine-grained region at the bottom of the sample. In addition, these fine grains were converted into nanotwinned columnar grains with a (111) orientation. The electroplated Cu film possessed extremely high (111) preferred orientation after the annealing.

© 2014 Acta Materialia Inc. Published by Elsevier Ltd. All rights reserved.

**Keywords:** Grain growth; Nanotwinned Cu; Preferred orientation; Electroplated Cu

Nanotwinned Cu (nt-Cu) has attracted a lot of attention in recent years because it has a higher strength than regular Cu, but possesses the same resistivity as bulk Cu [1]. Cu is the most important material for interconnects in the microelectronics industry. If the grain structure can transform into nanotwinned columnar grains, the electromigration resistance of the interconnect would increase. This effect is beneficial in Cu interconnects because twin boundaries are low-diffusivity paths [2,3]. Chen et al. observed a triple point where a twin boundary meets a grain boundary that can slow down grain-boundary electromigration by one order of magnitude [4]. Liu et al. also reported in their paper that a nanotwin can inhibit the formation of Kirkendall voids [5]; thus, nt-Cu has many advantages and is the best material for interconnects and under-bump metallurgy in microelectronic products.

Generally, a metal must be annealed after plating. However, annealing may induce grain growth. Therefore, the thermal stability of the metal is very important [6]. In a study by Anderoglu et al., nt-Cu was reported to exhibit excellent thermal stability; there was no seed layer on the substrate, the average grain size of the sputtered nt-Cu was 50 nm, the twin spacing was 5 nm, and after annealing at 800 °C, the twin structure still existed [7]. However, their nt-Cu was grown by sputtering and

thus cannot be used in microelectronic devices due to the manufacturing process and cost. Hsiao et al. published a method to deposit high-density nt-Cu by electroplating [8], which can be used in microelectronic devices. In their study, Cu was analyzed using X-ray diffraction (XRD), and the results revealed a significant (111)-preferred orientation. Such nt-Cu with preferred orientation can be used for Cu interconnects to improve their electromigration resistance [9,10] and for microbumps in 3-D integrated circuits. The results by electron backscattered diffraction (EBSD) analysis in the paper by Lin et al. revealed that after reflow soldering, the Cu<sub>6</sub>Sn<sub>5</sub> intermetallic compound in microbumps with a (111) nt-Cu/SnAg/(111) nt-Cu structure exhibited a particular preferred orientation, satisfactory mechanical and electromigration properties, and thus predictable reliability and failure modes [11]. However, in this type of nt-Cu, a layer of a fine-grained region near the seed layer is present, as illustrated in Figure 1a, resulting in a less consistent Cu structure. However, limited studies have been conducted on the thermal stability of electroplated Cu with a (111)-oriented nanotwinned structure.

In the present paper, the objective was to deposit (111)-oriented nt-Cu on a Si/Ti/Cu substrate using pulsed plating. In addition, after annealing at 250 °C for 1 h, the nanotwinned columnar grains on top grew downward, converting the original fine-grained region at the bottom into (111)-oriented nanotwinned columnar grains.

\* Corresponding author. Tel.: +886 3 5731814; fax: +886 3 5724727; e-mail: [chih@mail.nctu.edu.tw](mailto:chih@mail.nctu.edu.tw)

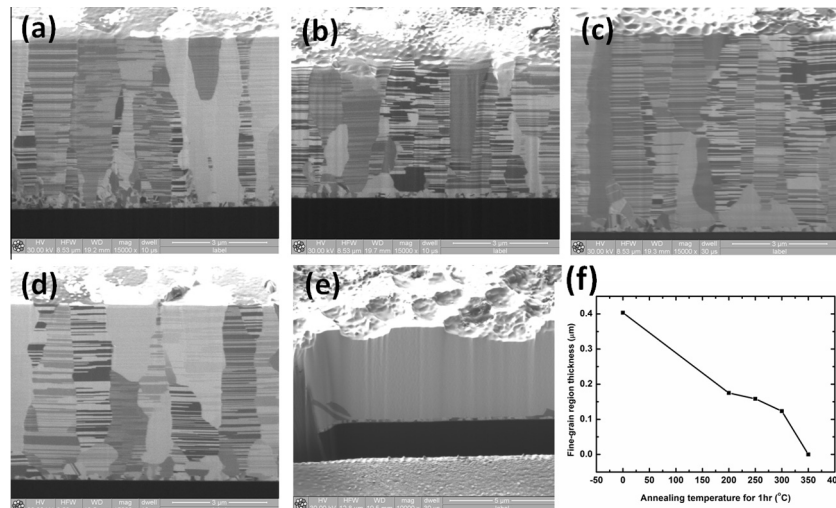


**Figure 1.** Cross-sectional FIB images for the nt-Cu after annealing at various temperatures: (a) as-plated; (b) 200 °C for 1 h; (c) 250 °C for 1 h; (d) 300 °C for 1 h; (e) 350 °C for 1 h; (f) measured thickness of the fine-grained region at the bottom of the Cu films.

The preparation of (111)-oriented nt-Cu involved the following steps: on a Si substrate, 100 nm (thickness) of Ti was sputtered as the barrier layer, and then 200 nm (thickness) of Cu was sputtered as the seed layer. The Cu seed layer had a (111)-preferred orientation [8]. The composition of the electroplating bath was as described in our previous studies. The electroplating bath was a high-purity  $\text{CuSO}_4$  solution composed of 0.8 M Cu cations, 40 ppm HCl and surfactants [12]. (111)-preferred oriented nt-Cu was plated by pulse plating. In each cycle of the pulsed plating, the plating was turned on with a  $50 \text{ mA cm}^{-2}$  current density for 1 s, i.e.,  $T_{\text{on}} = 1 \text{ s}$ , and then, the current density was decreased to 0, and the plating was turned off for 4 s, i.e.,  $T_{\text{off}} = 4 \text{ s}$ . The stirring speed of the electrolyte was 600 rpm. After 1000 cycles of plating, 7  $\mu\text{m}$  of (111) nt-Cu was produced. The plated samples were then annealed in a tube furnace at  $10^{-3}$  Torr and 200, 250, 300 or 350 °C for 1 h, followed by grinding. Later, the samples were etched in a FEI Nova 200 dual-beam focused ion beam (FIB) and scanning electron microscopy (SEM) system to flatten the surface. The grain growth in the samples was examined. To examine the orientation of the grains, EBSD analysis was performed using a JEOL7001 field emission scanning electron microscope with an EDAX electron backscatter diffraction system. Transmission electron microscopy (TEM) was employed to examine the structure of nanotwinned Cu.

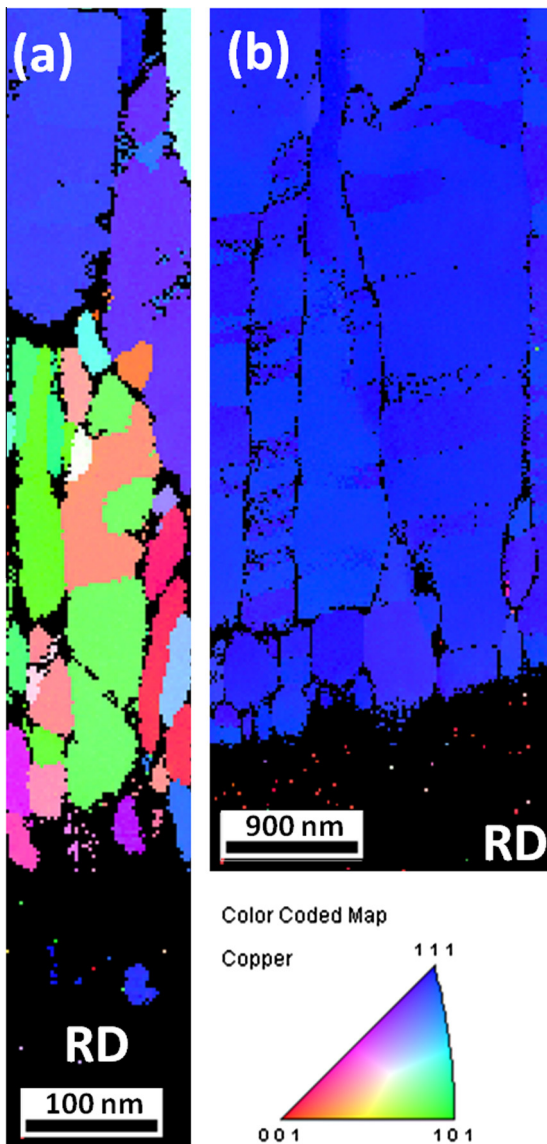
We observed that the annealed columnar grains with nt-Cu grew downward and converted the fine-grained region into the same structure (nanotwinned columnar grains). The grain growth is illustrated in Figure 1. Each sample was polished using FIB, and the cross-section was observed with ion imaging. Figure 1a presents an image of the as-plated sample. A 0.40  $\mu\text{m}$  thick fine-grained region was present above the seed layer at the bottom, and columnar Cu grains were present on the top, with an average grain size of  $0.5 \pm 0.1 \mu\text{m}$ , which represents a high-density nanotwinned structure. Changes in the annealed sample were observed:

Figure 1b presents an image of the sample annealed at 200 °C for 1 h. The results indicate that columnar grains with a high-density nanotwinned structure still existed, with the average grain size slightly increasing to  $0.6 \pm 0.1 \mu\text{m}$ . The thickness of the fine-grained region significantly decreased, and the fine-grained region at the bottom was transformed into a twinned structure. The thickness of the fine-grained region was measured to be 0.18  $\mu\text{m}$ . After annealing the samples at 250 °C for 1 h, the average size of the columnar grains was  $0.7 \pm 0.1 \mu\text{m}$ , and the conversion of the fine-grained region into columnar grains was more significant. As observed in Figure 1c, almost the entire fine-grained region had transformed into a twinned structure, and the thickness of the fine-grained region was 0.16  $\mu\text{m}$ . The seed layer with finer grains is the lowest layer, which was not converted. Mahajan et al. reported in their paper that the driving force to generate an annealing twin was larger when the Cu grain curvature was smaller, and the formation of annealing twins also helps to reduce the grain boundary energy [13]. After annealing, the columnar grains on top grew downward until the fine grains were completely consumed, and a nanotwinned columnar structure formed. Figure 1d presents an image of the sample after annealing at 300 °C for 1 h. The figure reveals that the columnar structure and twins remained, the average grain size increased to  $0.9 \pm 0.1 \mu\text{m}$ , and the fine-grained region was converted into columnar grains with nanotwins. At this time, the thickness of the fine-grained region was 0.12  $\mu\text{m}$ . Significant changes in the grain structure occurred when the annealing temperature was increased to 350 °C. Figure 1e presents an image of the sample after annealing at 350 °C for 1 h. The figure shows a significantly enlarged grain, and fine grains were still present in the seed layer, while the other pulsed-plated nt-Cu had all disappeared. This result indicates that the nanotwin in the nt-Cu deposited by pulse plating in our study was stable until the temperature increased to 350 °C. The measurements of the fine-grained region thickness at each stage are shown in Figure 1f. The fine-grained

region decreased with increasing annealing temperature. In addition, comparing our results with the results of Anderoglu et al., the structure of their sputtered Cu was completely columnar nt-Cu without the fine-grained region adjacent to see the seed layer, and their results revealed that the sputtered nt-Cu still existed after annealing at 800 °C, indicating that the stability is related to the method of deposition. [7]

To confirm the grain orientation of the samples, we performed EBSD analysis on the grain orientation of the nt-Cu in samples annealed at 250 °C, as shown in Figure 2. Figure 2a shows the grain orientation of the as-plated sample. This figure clearly demonstrates that the fine-grained region is composed of grains of various colors. Based on the color-coded map, the grains in this region are randomly oriented without a preferred orientation. The analysis results indicate that the proportion of (111)-oriented area was 43.3%. Figure 2b presents

the results for the sample annealed at 250 °C, which reveal that the grain color in the fine-grained region was all transformed to blue, indicating that the



**Figure 2.** Cross-sectional EBSD image for the fine-grained region: (a) as-plated and (b) after annealing at 250 °C for 1 h with a scanning step size of 0.02 μm.

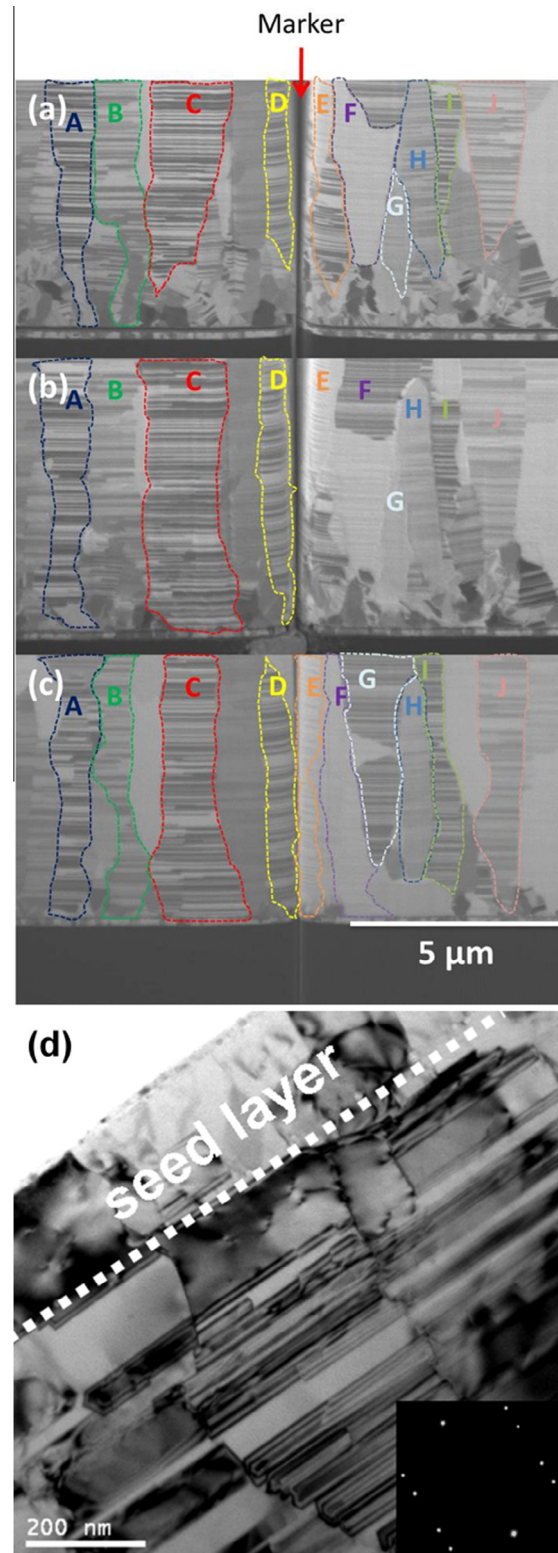


**Figure 3.** Microstructure evolutions on grains A–J before and after the annealing at 250 °C for 1 h: (a) before annealing; (b) after annealing; (c) after annealing and with a surface polishing by FIB; (d) cross-sectional TEM image on the nanotwinned Cu adjacent to the Cu seed layer.

annealing was conducive to converting this region into grains with (111)-preferred orientation. The analysis results indicate that the proportion of (111)-oriented area was 99.8%.

It is intriguing that not only the randomly oriented fine grains were converted into (111) large grains, but also the large grains in the bottom grew densely packed nanotwins after annealing at 250 °C for 1 h. In Figure 1a–d, it is observed that the (111) columnar grains consumed the tiny randomly oriented grains at the bottom, and the (111) columnar grains also had nanotwinned at the bottom. Yet, these are four different specimens. Thus, it is not convincing to state that the fine grains were converted into nanotwinned columnar grains. To provide direct evidence, we investigated the microstructure changes in the same area before and after the annealing. First, we used FIB to cut a cross-section on the (111)-oriented nt-Cu film, and etched a marker on the film. In this way, we can examine the microstructure evolutions of many specific grains before and after the annealing, as shown in Figure 3. Figure 3a,b presents the microstructure evolution on the grains A–J before and after the annealing at 250 °C for 1 h. To facilitate the observation of the grains, the grain boundaries were marked by dashed lines with different colors. For the nt-Cu films before annealing, there were many fine grains at the bottom of the film. However, after the annealing, it is very clear that the large nanotwinned grains A, B and C grew downward to consume the fine grains below them, and densely packed nanotwins also formed in the same time. We also polished the surface slightly by FIB, and we can observe other grains more clearly, as illustrated in Figure 3c. We can observe similar results for grains D–J. These results indicate that the fine grains were converted into nanotwinned columnar grains. These newly grown nanotwins were annealing twins, whereas the nanotwins in the as-plated Cu are growth twins. To further examine the structure of the annealing twins, FIB was employed to cut a TEM specimen near the Cu seed layer. Figure 3d presents the cross-sectional TEM image for the sample after the annealing at 250 °C for 1 h. The diffraction pattern in this region was shown in the inset and twin spots were observed. The 200 nm thick Cu seed layer was labeled in the figure. Densely packed nanotwins were observed in the Cu film adjacent to the seed layer. These twins belong to annealing twins. The average twin spacing was measured to be 60 nm.

The above FIB, TEM and EBSD results demonstrate that a moderate annealing temperature can cause the randomly oriented grains at the bottom to be replaced with (111)-oriented columnar nanotwinned grains. Therefore, performing moderate annealing after plating the film can convert the entire film into (111)-oriented columnar nanotwinned grains. For the formation mechanism for annealing nanotwins, it is well known that Cu has a low stacking fault energy [1]. The formation of the coherent nanotwins at this temperature may increase the entropy and reduce the free energy. In addition, when the

large columnar grains consume the randomly oriented small grains, many grain boundaries will be annihilated and thus it is an energetic favorably process. Nevertheless, further theoretical calculations need to be performed to verify the free energy reduction.

In summary, nt-Cu with a (111)-preferred orientation was electroplated by pulse plating. The samples were annealed at 200, 250, 300 and 350 °C. For the samples annealed at temperatures below 300 °C, the sample annealed at 250 °C for 1 h exhibited the highest I(111)/I(200) peak intensity ratio, indicating that this sample had the strongest (111)-preferred orientation. In addition, the EBSD analysis results indicate that the fine-grained region adjacent to the seed layer was randomly oriented immediately after plating. Two changes were observed after annealing: first, the initially random orientation was transformed into a highly (111)-preferred orientation. Second, the original fine grains were converted into larger columnar grains with a nanotwinned structure. These are new findings and will have an impact in the field of grain growth of nanotwinned materials.

Financial support from the National Science Council, Taiwan, under the contracts NSC 99-2221-E-009-040-MY3, is acknowledged. The authors would like to thank the Center for Micro/Nano Science and Technology (CMNST) at National Cheng Kung University for assistance with the analytical equipment.

- [1] L. Lu, Y.F. Shen, X.H. Chen, L.H. Qian, K. Lu, *Science* 304 (2004) 422–426.
- [2] R. Rosenberg, D.C. Edelstein, C.K. Hu, K.P. Rodbell, *Annu. Rev. Mater. Sci.* 30 (2000) 229–262.
- [3] D. Xu, V. Sriram, V. Ozolins, J.M. Yang, K.N. Tu, G.R. Stafford, C. Beauchamp, I. Zienert, H. Geisler, P. Hofmann, E. Zschech, *Microelectron. Eng.* 85 (2008) 2155–2158.
- [4] K.C. Chen, W.W. Wu, C.N. Liao, L.J. Chen, K.N. Tu, *Science* 321 (2008) 1066–1069.
- [5] T.C. Liu, C.M. Liu, Y.S. Huang, C. Chen, K.N. Tu, *Scripta Mater.* 68 (2013) 241–244.
- [6] J.M.E. Harper, C. Cabral Jr., P.C. Andricacos, L. Gignac, I.C. Noyan, K.P. Rodbell, C.K. Hu, *J. Appl. Phys.* 86 (2009) 2516–2525.
- [7] O. Anderoglu, A. Misra, H. Wang, X. Zhang, *J. Appl. Phys.* 103 (2008) 009432.
- [8] H.Y. Hsiao, C.M. Liu, H.W. Lin, T.C. Liu, C.L. Lu, Y.S. Huang, C. Chen, K.N. Tu, *Science* 336 (2012) 1007–1010.
- [9] C. Ryu, A.L.S. Loke, T. Nogami, S.S. Wong, in: 35th Annu. IEEE Int. Reliability Phys. Symp. Proc., 1997, pp. 201–205.
- [10] K.N. Chen, A. Fan, C.S. Tan, R. Reif, *Appl. Phys. Lett.* 81 (2002) 3774–3776.
- [11] H.W. Lin, C.L. Lu, C.M. Liu, C. Chen, D. Chen, J.C. Kuo, K.N. Tu, *Acta Mater.* 61 (2013) 4910–4919.
- [12] T.C. Liu, C.M. Liu, H.Y. Hsiao, J.L. Lu, Y.S. Huang, C. Chen, *Cryst. Growth & Des.* 12 (10) (2012) 5012–5016.
- [13] S. Mahajan, C.S. Pande, M.A. Imam, B.B. Rath, *Acta Mater.* 45 (1997) 2633–2638.